10.1098/rsta.2003.1209

THE ROYAL SOCIETY

Oxford ion-trap quantum computing project

By D. M. Lucas, C. J. S. Donald, J. P. Home, M. J. McDonnell, A. Ramos, D. N. Stacey, J.-P. Stacey, A. M. Steane and S. C. Webster

Centre for Quantum Computation, University of Oxford, Clarendon Laboratory, Parks Road, Oxford OX1 3PU, UK

We describe recent progress in the development of an ion-trap quantum information processor. We discuss the choice of ion species and describe recent experiments on read-out for a ground-state qubit and photoionization trap loading.

Keywords: ion traps; quantum computing; photoionization

1. Introduction

The ion trap is regarded as one of the most promising systems in which to implement a small-scale quantum information processor, and deterministic entanglement of up to four particles has already been demonstrated in this system (Sackett *et al*. 2000). Although the original architecture of Cirac & Zoller (1995) appeared to be limited in its prospects for scalability to large numbers of qubits, proposals for multiple ion traps circumvent this problem (Kielpinski *et al*. 2002) and recent experiments on the 'unit cell' of such a system indicate the feasibility of this approach (Rowe *et al*. 2002).

In this paper we describe an ion-trap project at the Centre for Quantum Computation at Oxford, whose goal is a small-scale quantum information processor. We describe initial experiments on read-out (state detection) for a qubit encoded in the ground level of the $^{40}Ca^{+}$ ion, and outline future plans for qubits encoded in hyperfine states of the $^{43}Ca^{+}$ ion. We begin by discussing the choice of ion species.

2. Choice of ion

There are many factors to consider in evaluating the suitability of different ions for quantum information processing experiments, some of which are listed in table 1, and there is no obvious optimum choice. These factors are both technical and fundamental. An important technical consideration is the complexity of the laser systems required for laser cooling, state preparation, gates and state detection. Most ions require frequency-doubled laser systems, which add both complexity and intensity noise to the system; the latter makes the generation of, for example, accurate π-pulses more difficult. Fundamental constraints are imposed by the physical properties of the

One contribution of 20 to a Discussion Meeting 'Practical realizations of quantum information processing'.

ion; these may limit, for example, how efficiently it is possible to detect the state of an ion qubit with a single measurement, or the fidelity of a particular gate implementation.

An important limitation for gates based on Raman transitions between qubit states is given by off-resonant one-photon excitation: even a single scattered photon will corrupt the qubit state with high probability. Since, for a Raman detuning from an allowed transition Δ, the two-photon transition rate is proportional to $1/\Delta$, whereas the one-photon rate is proportional to $1/\Delta^2$, it is advantageous to increase Δ. However, once Δ is made large compared with the fine-structure splitting Δ_{FS} (table 1) the two-photon transition rate tends to zero because of cancellations in the contributions from the two upper levels. The situation is treated in detail by Wineland *et al.* (2003), but a simple figure of merit (table 1) is given by the ratio of the fine-structure splitting Δ_{FS} to the one-photon line width Γ: the larger the value of Δ_{FS}, the greater the possible Raman detuning; the smaller the line width Γ, the lower the one-photon scattering rate for a given Δ.

We see from table 1 that $^{43}\mathrm{Ca}^+$ is only middling in terms of this Raman-gate figure of merit. However, it offers the significant technical advantage that all the required laser wavelengths are directly available from solid-state-diode lasers, without the need for frequency-doubling; these lasers can be made very stable in intensity and are also cheap and convenient sources. Single $^{40}\mathrm{Ca}^+$ ions have been trapped in our apparatus for over a month, indicating a long lifetime against reaction with residual background gas: an important consideration for a system with many ion qubits. An apparent disadvantage is the existence of metastable D states, which require additional repumping lasers, but these can also allow very accurate detection of the qubit state using the technique of electron shelving (Nagourney *et al.* 1986). $^{87}\mathrm{Sr}^+$ shares some of these features, and has a somewhat better figure of merit, but the laser wavelengths required for photoionization (§ 4) are less convenient. The heavy ions $^{111}\mathrm{Cd}^+$ and $^{199}\mathrm{Hg}^+$ have the best figures of merit but require complex laser sources; the latter ion also needs a cryogenic vacuum system.

3. Read-out methods for a $^{40}\mathrm{Ca}^+$ ground-level qubit

The existing Oxford experiment uses $^{40}\mathrm{Ca}^+$ ions in a linear ion trap; relevant energy levels are shown in figure 1*a*. For first experiments, we intend to use the $\mathrm{S}_{1/2}^{\pm 1/2}$ Zeeman states of the ground level (where the superscript denotes M_J) for the internal qubit states. These states are extremely long-lived, and Raman transitions between them can be used for sideband cooling, single-qubit manipulations and entangling the internal and motional states of ions. The energy separation between the two states is determined by an applied magnetic field, typically chosen to be small (*ca.* 5 G) so that field-fluctuations are minimized. Unfortunately, this means that it is difficult to discriminate between the two states to 'read out' the state of the qubit, because the energy separation is small compared with the line widths of allowed electric-dipole transitions from the qubit states. In order to take advantage of the high detection efficiency offered by electron shelving, we need to map selectively one of the qubit states onto the metastable $\mathrm{D}_{5/2}$ level. This level does not fluoresce in the normal $\mathrm{S}_{1/2} \leftrightarrow \mathrm{P}_{1/2} \leftrightarrow \mathrm{D}_{3/2}$ laser-cooling cycle so that it is straightforward to detect whether or not the ion has been shelved. Two possible methods of achieving

Table 1. *Data for some candidate qubit ions*

(The third and fourth columns give the wavelengths of the S–P transition used for cooling/shelving and the D–P transition used for repumping those ions which have low-lying D-states. The last three columns give the fine structure splitting Δ_{FS} of the P term, the S–P line width Γ and their ratio.)

ion	nuclear spin, $\hbar$	$S_{1/2}$–$P_{3/2}$ λ (nm)	$D_{3/2}$–$P_{1/2}$ λ (nm)	$P_{3/2}$–$P_{1/2}$ splitting Δ_{FS} (THz)	$S_{1/2}$–$P_{3/2}$ line width Γ (MHz)	$\Delta_{\mathrm{FS}}/\Gamma$ ($/10^6$)
$^{9}Be^{+}$	3/2	313	—	0.20	20	0.010
$^{25}Mg^{+}$	5/2	280	—	2.7	43	0.063
$^{43}Ca^{+}$	7/2	393	866	6.7	23	0.29
$^{87}Sr^{+}$	9/2	408	1 092	24	23	1.0
$^{111}Cd^{+}$	1/2	215	—	75	47	1.6
$^{199}Hg^{+}$	1/2	194	(10 700)	274	69	4.0

the required mapping are outlined below. (Note that an alternative choice of qubit in $^{40}Ca^{+}$, which does not require this mapping, is described in Nägerl *et al.* (2000).)

(*a*) *High-field read-out*

A simple method to shelve one of the $S_{1/2}^{\pm 1/2}$ qubit states is to increase the magnetic field until the various Zeeman components of the $S_{1/2} \leftrightarrow P_{3/2}$ transition are spectrally well-resolved. Driving the $S_{1/2}^{-1/2} \leftrightarrow P_{3/2}^{-3/2}$ cycling transition then transfers the ion from the $S_{1/2}^{-1/2}$ state to the $D_{5/2}$ 'shelf', without affecting the $S_{1/2}^{+1/2}$ state (figure 1*a*). Due to a favourable branching ratio to the $D_{5/2}$ level this occurs with a probability of *ca.* 89% in the limit of large magnetic field (*ca.* 200 G). This method was suggested by Stevens *et al.* (1998) and we have since implemented it (Lucas 2001); experimental results for the read-out efficiency are shown in figure 1*b*. The optimum experimental read-out efficiency achieved was only *ca.* 65% and appeared to be limited by instabilities associated with the rapid switching of the large magnetic field. Since a stable magnetic field is required to preserve qubit phases, this method seems likely to be unsatisfactory in the long term.

(*b*) *'Raman' read-out*

Two-photon transitions can provide much narrower resonances than one-photon transitions, for example in the well-known phenomenon of dark and bright resonances (Siemers *et al.* 1992). It is possible to use these narrow spectral features to discriminate between the $S_{1/2}^{\pm 1/2}$ qubit states at low magnetic field, without having to increase their energy separation. A possible scheme involves two lasers detuned from the $S_{1/2} \leftrightarrow P_{3/2}$ transition and the $D_{3/2} \leftrightarrow P_{3/2}$ transition (figure 2*a*), such that the Raman

$$S_{1/2}^{-1/2} \Leftrightarrow D_{3/2}^{-1/2}$$

transition gives a dark resonance, while the

$$S_{1/2}^{+1/2} \Leftrightarrow D_{3/2}^{+1/2}$$

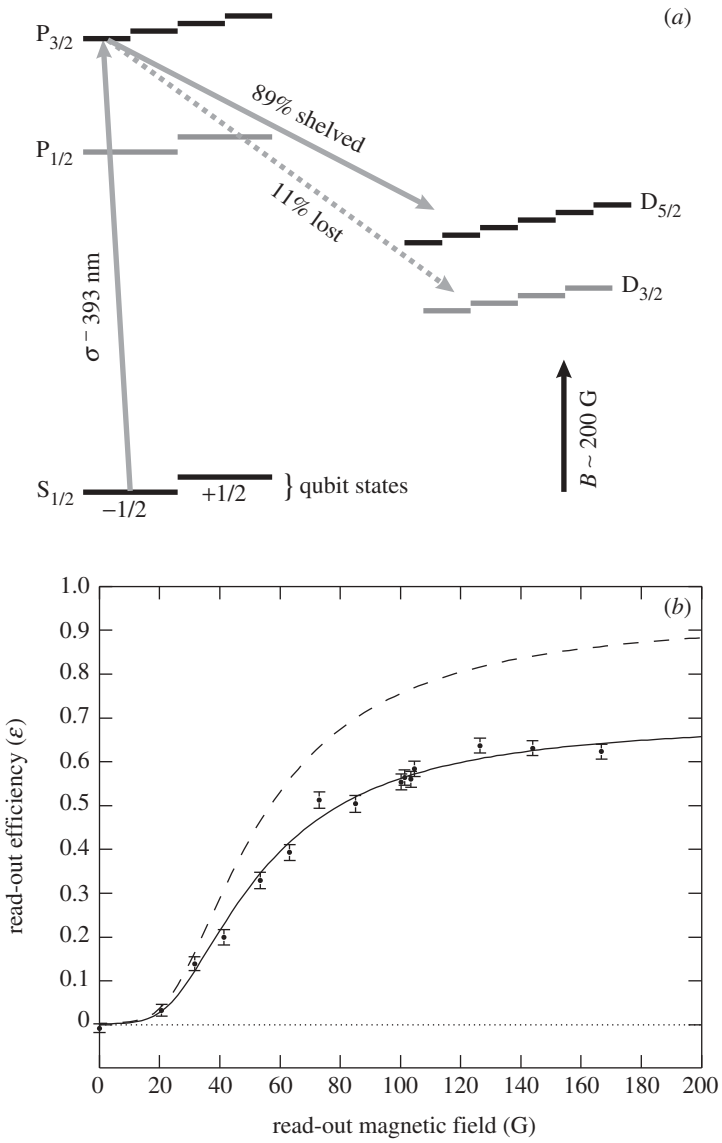

Figure 1. (*a*) $^{40}Ca^{+}$ energy levels and the high-field read-out method. The large (*ca.* 200 G) magnetic field allows the 393 nm $S_{1/2}^{-1/2} \leftrightarrow P_{3/2}^{-3/2}$ cycling transition to be resolved from the $S_{1/2}^{+1/2} \leftrightarrow P_{3/2}^{-1/2}$ transition, in order that the qubit state $S_{1/2}^{-1/2}$ can be selectively shelved in the metastable $D_{5/2}$ state by a short 393 nm σ^{-} laser pulse. (*b*) High-field read-out results. The read-out efficiency ϵ is defined as the probability of shelving when the ion is prepared in the $S_{1/2}^{-1/2}$ state minus the probability of shelving when the ion is prepared in the $S_{1/2}^{+1/2}$ state. The solid line is a fit of the expected efficiency based on a rate equation model, where the fitted parameters are the 393 nm laser intensity and the initial populations. From this fit we find that the efficiency does not reach the expected level (dashed line) because of imperfect preparation of the initial states; we attribute this to fluctuations in the low magnetic field used during the state-preparation phase caused by the switching of the high field.

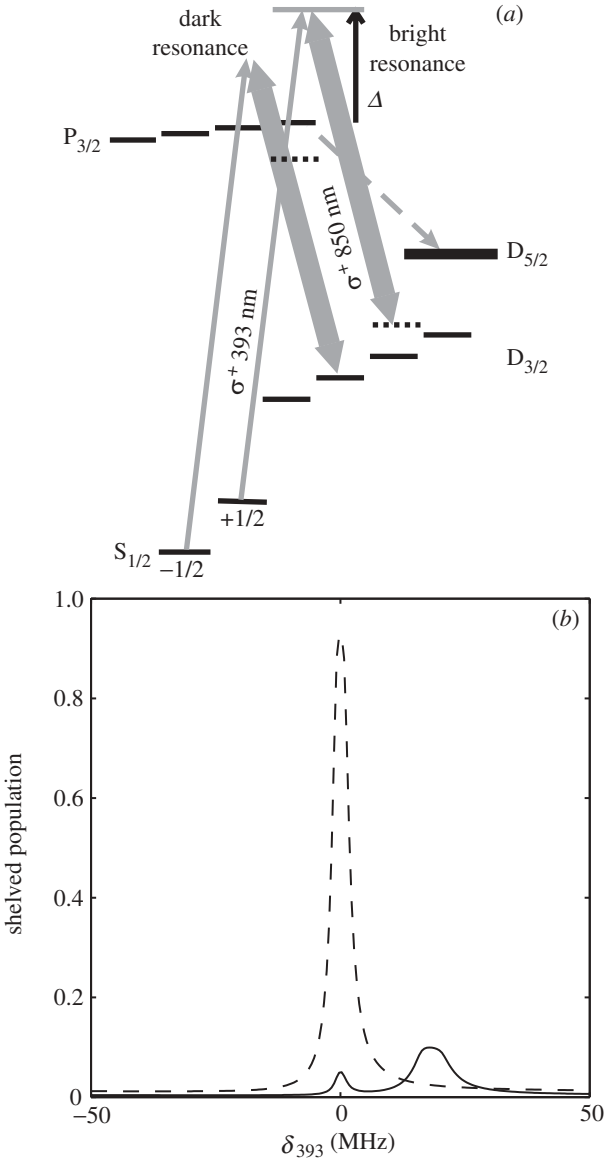

Figure 2. (*a*) Mechanism for shelving the $S_{1/2}^{+1/2}$ qubit state using a two-photon bright resonance. Two lasers are involved, an intense infrared laser detuned from the 850 nm $D_{3/2} \leftrightarrow P_{3/2}$ transition by $\Delta \sim 1$ GHz and a weak violet laser detuned from the 393 nm $S_{1/2} \leftrightarrow P_{3/2}$ transition by $(\Delta + \delta_{393})$. Dotted lines indicate light-shifted levels. For a given power in the 850 nm laser the (few Gauss) magnetic field can be chosen so that the bright resonance of the $S_{1/2}^{+1/2} \Leftrightarrow D_{3/2}^{+1/2}$ Raman transition coincides with a dark resonance of the $S_{1/2}^{-1/2} \Leftrightarrow D_{3/2}^{-1/2}$ transition, so that the $S_{1/2}^{-1/2}$ state is unaffected, while the $S_{1/2}^{+1/2}$ state is transferred to the $D_{5/2}$ 'shelf'. (*b*) Theoretical calculations of the shelved population as a function of δ_{393} for an ion in the initial state $S_{1/2}^{+1/2}$ (dashed line) and for an ion in the initial state $S_{1/2}^{-1/2}$ (solid line). This calculation takes into account the effect of finite laser line width (taken as 0.5 MHz for each laser), and gives a peak shelving efficiency of *ca.* 88%.

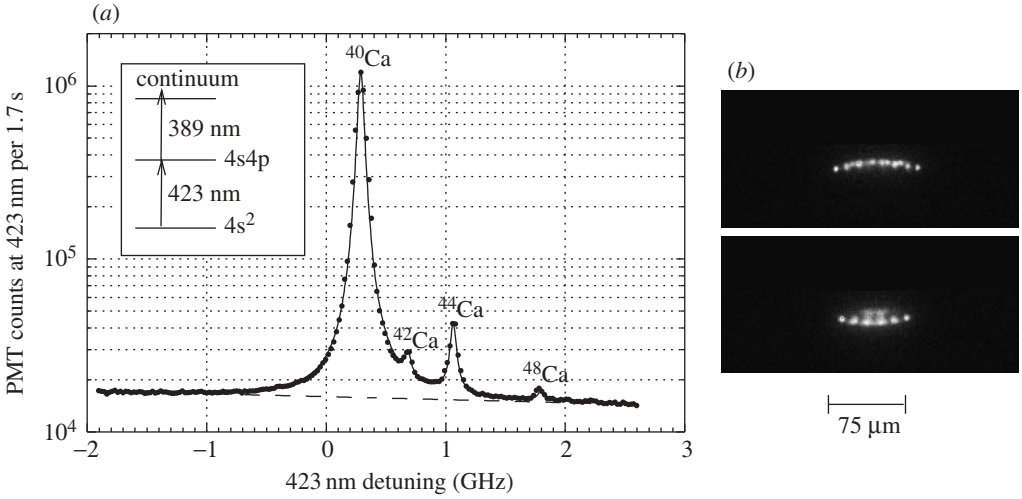

Figure 3. (*a*) The inset shows the levels involved in two-step resonance photoionization of neutral calcium. The main graph shows the fluorescence observed on the 423 nm transition, using the ion-trap photomultiplier system, as a function of 423 nm laser detuning. The atomic beam is collimated by the trap electrode structure and the 423 nm laser beam intersects the atomic beam at right angles, making the Doppler width comparable with the natural line width $\Gamma = 35$ MHz (a total full width at half maximum (FWHM) of *ca.* 75 MHz). A superposition of Lorentzian profiles, one for each of the even isotopes and the three hyperfine transitions of ^{43}Ca, is also plotted (solid line); it is given the known abundances and isotope shifts, and amplitude, offset, baseline and width to match the data approximately. The effect of the ^{43}Ca peaks is not visible on this scale, but is just detectable in the data; however, an enriched source will be needed for reliable loading of this isotope. (*b*) A mixed-species crystal of $^{40}Ca^{+}$ and $^{44}Ca^{+}$ ions, loaded using photoionization and observed by the ion-trap camera system. The Doppler-cooling lasers are tuned close to resonance with the $^{40}Ca^{+}$ transitions in the top picture (and the $^{44}Ca^{+}$ ions are not visible), and vice versa in the bottom picture.

transition exhibits a bright resonance. The dark resonance means that the $S_{1/2}^{-1/2}$ state is unaffected, while the $S_{1/2}^{+1/2}$ state Rabi-flops to the $D_{3/2}^{+1/2}$ state, whence it can be partly excited to $P_{3/2}^{+3/2}$ and will eventually decay to the $D_{5/2}$ 'shelf'. In this scheme the shelving efficiency can in principle be made close to 100% by careful control of the laser polarizations. In practice, factors such as imperfect laser polarization and finite laser line width reduce the efficiency, but the 90% level should not be difficult to achieve; a theoretical calculation taking these factors into account is shown in figure 2*b*, and experiments are in progress.

4. $^{43}Ca^{+}$ and photoionization trap loading

The difficulties associated with read-out in $^{40}Ca^{+}$ make the use of the odd isotope $^{43}Ca^{+}$ attractive: the moderately large (*ca.* 3.2 GHz) ground-state hyperfine splitting present in $^{43}Ca^{+}$ retains the advantage of long-lived states accessible to Raman transitions while simplifying the problem of state discrimination. The hyperfine structure also offers $M_F = 0$ states which may be useful in the long term because of their first-order insensitivity to fluctuations in the applied magnetic field.

The most obvious difficulty in working with $^{43}Ca^{+}$ is the low natural isotopic abundance of 0.14%. Since the maximum isotopic enrichment available is *ca.* 80%, it will be advantageous to use an isotope-selective method to load the ion trap reliably with $^{43}Ca^{+}$. Photoionization has been successfully used to load different isotopes of calcium into an ion trap by Kjaergaard *et al.* (2000) and also has technical advantages over the usual ionization method of electron bombardment: like Gulde *et al.* (2001), we have found that drifting offset fields caused by firing the electron beam are eliminated, and that the significantly more efficient process of photoionization means that the neutral atomic beam density can be much reduced (which should reduce deposition on the trap electrodes and associated heating (Turchette *et al.* 2000)).

We can clearly distinguish the different even isotopes in the neutral calcium $4s^2 \leftrightarrow 4s4p$ fluorescence spectrum at 423 nm (figure 3*a*). To ionize the neutral atoms, (non-resonant) excitation from the 4s4p level to the continuum is provided by a free-running laser diode operating at 388.9 nm (the ionization limit requires $\lambda < 389.8$ nm, but in any case the continuum edge is broadened by the electric fields from the trap). By setting the detuning of the grating-stabilized 423 nm laser appropriately we have loaded the ion trap with $^{40}Ca^{+}$, $^{42}Ca^{+}$, $^{44}Ca^{+}$ or $^{48}Ca^{+}$ ions. Figure 3*b* shows a mixed crystal of $^{40}Ca^{+}$ and $^{44}Ca^{+}$ isotopes.

5. Conclusion

We have summarized the current status of the Oxford ion-trap project, including recent experiments on read-out of a ground-state qubit and photoionization trap loading. The choice of $^{43}Ca^{+}$ as a suitable ion for quantum information experiments has been explained as offering a good compromise between technical complexity and the fidelity of gate operations carried out using Raman transitions. We note that gates do not necessarily have to be based on Raman transitions: an example is the so-called 'pushing gate' proposed by Cirac & Zoller (2000). Recent detailed calculations on this gate (Šašura & Steane 2003) indicate that it is capable of providing high fidelity at reasonable speed without the need for ground-state cooling.

We are grateful for the technical assistance of Graham Quelch. The Raman read-out scheme described in § 3 *b* was conceived by Matt McDonnell, following the EIT-cooling ideas of Morigi *et al.* (2000). The research is supported by ARDA, EPSRC, the EU and The Royal Society.

References

Cirac, J. I. & Zoller, P. 1995 Quantum computations with cold trapped ions. *Phys. Rev. Lett.* **74**, 4091–4094.

Cirac, J. I. & Zoller, P. 2000 A scalable quantum computer with ions in an array of microtraps. *Nature* **404**, 579–581.

Gulde, S., Rotter, D., Barton, P., Schmidt-Kaler, F., Blatt, R. & Hogervorst, W. 2001 Simple and efficient photoionization loading of ions for precision ion-trapping experiments. *Appl. Phys.* B **73**, 861–863.

Kielpinski, D., Monroe, C. & Wineland, D. J. 2002 Architecture for a large-scale ion-trap quantum computer. *Nature* **417**, 709–711.

Kjaergaard, N., Hornekaer, L., Thommesen, A. M., Videsen, Z. & Drewsen, M. 2000 Isotope selective loading of an ion trap using resonance-enhanced two-photon ionization. *Appl. Phys.* B **71**, 207–210.

Lucas, D. M. 2001 Development of a linear ion trap for quantum computing. In *Proc. First Int. Conf. on Experimental Implementations of Quantum Computers, Sydney, Australia, 2001*, pp. 91–98. Princeton: Rinton Press.

Morigi, G., Eschner, J. & Keitel, C. H. 2000 Ground-state laser cooling using electromagnetically induced transparency. *Phys. Rev. Lett.* **85**, 4458–4461.

Nägerl, H. C., Roos, C., Leibfried, D., Rohde, H., Thalhammer, G., Eschner, J., Schmidt-Kaler, F. & Blatt, R. 2000 Investigating a qubit candidate: spectroscopy on the $S_{1/2}$ to $D_{5/2}$ transition of a trapped calcium ion in a linear Paul trap. *Phys. Rev.* A **61**, 023405.

Nagourney, W., Sandberg, J. & Dehmelt, H. 1986 Shelved optical electron amplifier: observation of quantum jumps. *Phys. Rev. Lett.* **56**, 2797–2799.

Rowe, M. A. (and 12 others) 2002 Transport of quantum states and separation of ions in a dual RF ion trap. *Quant. Informat. Computat.* **2**, 257–271.

Sackett, C. A. (and 10 others) 2000 Experimental entanglement of four particles. *Nature* **404**, 256–258.

Siemers, I., Schubert, M., Blatt, R., Neuhauser, W. & Toschek, P. E. 1992 The 'trapped state' of a trapped ion: line shifts and shape. *Europhys. Lett.* **18**, 139–144.

Stevens, D., Brochard, J. & Steane, A. M. 1998 Simple methods for trapped-ion quantum information processors. *Phys. Rev.* A **58**, 2750–2759.

Turchette, Q. A. (and 10 others) 2000 Heating of trapped ions from the quantum ground state. *Phys. Rev.* A **61**, 063418.

Šašura, M. & Steane, A. M. 2003 Fast quantum logic with selective displacement of hot trapped ions. *Phys. Rev.* A (Preprint quant-ph/0212005.)

Wineland, D. J. (and 10 others) 2003 Quantum information processing with trapped ions. *Phil. Trans. R. Soc. Lond.* A **361**, 000–000.